

An Advanced System for Vibration Control of Flexible Structures

A. Cavallo* G. De Maria* C. Natale* S. Pirozzi*

** Dipartimento di Ingegneria dell'Informazione
Seconda Università degli Studi di Napoli, Aversa, 81031 Italy
(e-mail: ciro.natale@unina2.it)*

Abstract: The objective of the research work here presented is the rejection of a broadband disturbance in a vibrating flexible structure. From a technological point of view, the problem is tackled using an advanced lightweight magnetostrictive resonant actuator with an integrated optical strain sensor. The adopted control strategy consists of a two-levels controller. Usefully exploiting the measurement of the integrated sensor, a low-level feedback loop, aimed at linearizing the actuator behaviour, is designed by resorting to a model-following approach. An optimal control law is specifically implemented as the high-level feedback loop providing a \mathcal{H}_∞ strongly stabilizing controller with bandpass capability for both low- and high-frequencies measurement disturbances affecting the accelerometer used as control sensor. The advanced control system has been experimentally tested on an aeronautical stiffened panel.

Keywords: Mechatronic systems; integrated sensors and actuators; multi sensor systems; transportation systems; optimal control

1. INTRODUCTION

The present work related to the MESEMA project, whose target is reported by Lecce et al. (2006), has the objective to prove an advanced control concept for the vibration reduction, relying on the use of an integrated actuator/sensor based on unconventional technologies. The problem to be addressed is the reduction of broadband vibrations on an aeronautical structure from 100 Hz to 400 Hz. Many researcher contributed to solve the active vibration control problem. The general approach consists in measuring a signal related to an undesired vibration and manipulate it by a controller, that in turn computes the corrective action to exert on the structure by means of one or more actuators in order to reduce the vibration.

The selection of the most appropriate actuator strongly depends on the force requirements in terms of force levels and frequency range in relation to the weight limitations which are very restrictive when aeronautical applications are considered. To tackle the vibration control presented in this paper, an actuator based on a proven and patented actuator concept by May et al. (2003), the magnetostrictive auxiliary mass damper (shown in Fig. 1) was selected. In order to satisfy both the force and the weight requirements, the actuator, even though optimally designed for the specific application by May et al. (2006), uses a non-linear amplification mechanism of the displacement which is a source of nonlinearity in the overall system. Therefore, a suitable control algorithm is necessary to counteract the undesired effects of this nonlinearity, e.g. excitation of high-frequency unmodelled structural dynamics or shift of the actuator resonant frequency. In order to implement the actuator controller by resorting to a feedback strategy, an innovative optical strain sensor based on a fibre Bragg grating (FBG) has been integrated into the actuator so as

to usefully exploit its advantages clarified by Kersey et al. (1997).

When model based approaches are used to tackle the control design phase for the vibration control problem discussed above, the question of a suitable modelling technique of the vibrating structure arises. Such systems are described by partial differential equations (PDE's), that can be suitably cast in a infinite set of ordinary differential equation (ODE's). Next, a model order reduction takes place, and a finite set of ODE's is deduced. This operation, however, generally involves truncation of the high frequency dynamics, whose effect must be negligible, otherwise "spillover" effects may appear (Balas, 1982). This can be obtained by "filtering out" high frequency dynamics, by employing low-pass filtering within the control action. Also low frequencies must be filtered out, otherwise the very low frequency components of the measured signal would saturate the actuators, thus resulting in a very poor control performance. Typical examples are the rigid-body dynamics, that is immaterial in vibration control and is obviously sensed by an accelerometer. In principle, the filtering capability of the controller can be arbitrarily imposed by employing a loop-shaping technique, but this techniques does not guarantee strong stabilization, i.e. stabilization with a stable controller. In practical implementation of the controller, strong stabilization is a crucial requirement, since unstable controllers may tend to saturate actuators during transient phases. Moreover, it is well known that unstable elements in the forward path degrade the performances of the control system (Skogestad and Postlethwaite, 2005). Stable stabilizing controllers have been discussed in the last years, mainly in the SISO case, starting from the paper by Youla et al. (1974) till the more recent solutions based on LMI's as

proposed by Gümüşsoy and Özbay (2005) or parametric optimization as by Campos-Delgado and K. (2003). A very effective solution applicable to the MIMO case appeared in 1994 (Halevi, 1994), when Halevi proposed a suitable selection of the weighting matrices for an LQG problem so as to achieve strong stability. All the above results aim at solving the problem in the general case, hence no closed-form solution is given. This is a strong limitation when the control of high-order systems is addressed, since numerical solution are often ill-conditioned hence the resulting controller is not implementable.

The control strategy selected to tackle both the problem of actuator control and vibration reduction consists of a multi-loop architecture, where the inner controller is designed so as to counteract the effects of the nonlinear behaviour of the smart actuator while the outer controller uses a robust control strategy to reject the primary disturbance field. In detail, a model-following control strategy inspired to the one proposed by Balestrino et al. (1984) making use of the displacement of the actuator's seismic mass measured through the FBG is adopted. The characteristic of the model-following algorithm consists in preserving the nature of the input signal of the low-level control system, which is the output of the high-level vibration control system. This part of the control algorithm is designed by following the approach of Cavallo et al. (2008), where a closed-form solution to a strongly stabilizing \mathcal{H}_2 and \mathcal{H}_∞ control problem is proposed. The effectiveness of the advanced control system has been demonstrated through experiments performed on a real aeronautical structure, i.e. an aluminium stiffened skin panel.

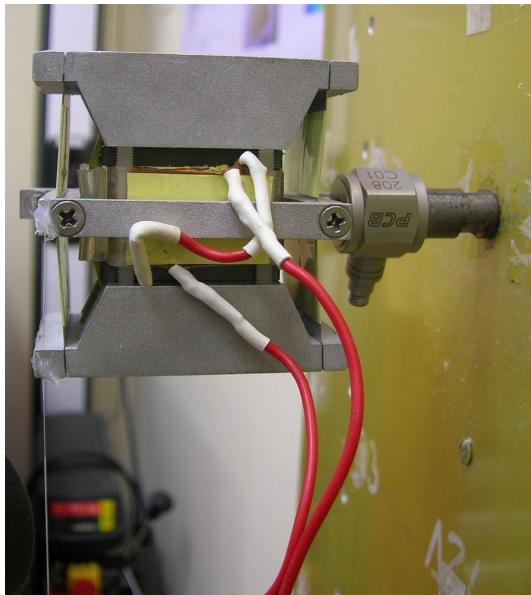


Fig. 1. Smart actuator mounted to the structure.

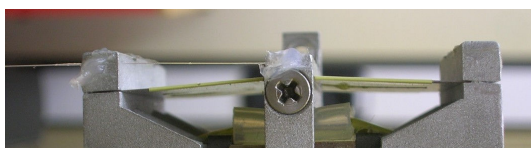


Fig. 2. Integrated optical sensor.

2. ADVANCED CONTROL SYSTEM

The control system for vibration reduction proposed in this paper has to be considered advanced in the sense that it makes use of an unconventional actuator based on a smart material with an integrated innovative optical sensor and of a hierarchical control architecture with two nested control loops. The objective of the inner controller, based on a model-following approach, is to reduce the undesired effects of the actuator nonlinearity. The outer controller, based on a \mathcal{H}_∞ robust control strategy, is devoted to achieve the main objective of reducing the disturbing vibrations. In the following subsections, technical details of each component of the advanced control system are presented.

2.1 Integrated Actuator/Sensor

Fig. 3 shows the fundamental construction inside the smart auxiliary mass damper designed and manufactured by May et al. (2003). It consists of magnetostrictive rods surrounded by two coils. The coils are on two backing plates that are connected with the stiff frame via two elastic suspensions arranged in parallel. The frame itself is mounted to the vibrating mechanical structure. Due to the magnetostrictive effect a magnetic field caused by a driving current in the coils produces a small extension in the magnetostrictive rods in the horizontal direction. This extension is transformed by the elastic suspensions to a significantly larger motion of the total mass –consisting of the magnetostrictive rods, the coils and the backing plates– in the perpendicular direction. The kinematics of the displacement amplification is strongly nonlinear and the amplification factor decisively depends on the angle of the elastic suspension at the working point α_0 of the mechanical construction (see Fig. 3), and is greater the smaller this angle α_0 is chosen. As a result of Newton's second law, the total moved mass produces an inertial force that has an effect on the vibrating mechanical structure (May et al., 2003, 2006).

With the objective of minimizing the nonlinear effects of the actuator using a feedback controller, an optical strain sensor has been integrated in the device to measure the displacement of the inertial mass, so as to estimate the state of the mechanical system. The sensor, based on a Fiber Bragg Grating (FBG), is sensitive to the strain of the optical fiber in which it is written. Therefore, by bonding the FBG between the backing plate and the fixation frame (see Fig. 1), the strain of the fiber is related to the displacement of the backing plate itself. Using a special optoelectronic circuit which interrogates the FBG in reflection mode, the sensed displacement can be converted into a voltage signal with an estimated sensitivity of about $37.6 \text{ mV}/\mu\text{m}$. For further details on the sensor integration and the interrogation technique, the interested reader is referred to the recent paper by May et al. (2007).

The most relevant effect of the actuator nonlinear kinematics when it is mounted to the vibrating structure is a dependence of the natural frequencies of the structure on the input current amplitude. This effect is particularly relevant in the frequency range close to the resonant frequency

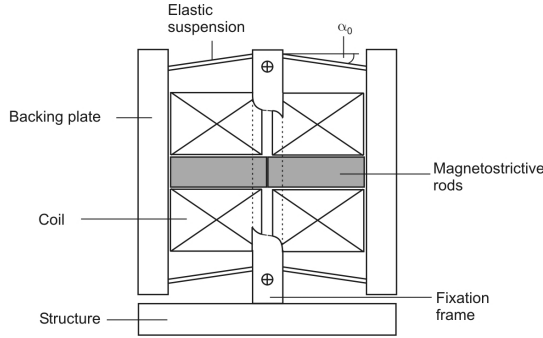


Fig. 3. Schematic design of the smart auxiliary mass damper.

of the actuator. Fig. 4 reports the frequency response function (FRF) measured from the input current to the optically sensed displacement using different amplitudes of the exciting chirp signal, i.e. 0.6, 1.2, 2 A. The shift of the natural frequencies appears evident.

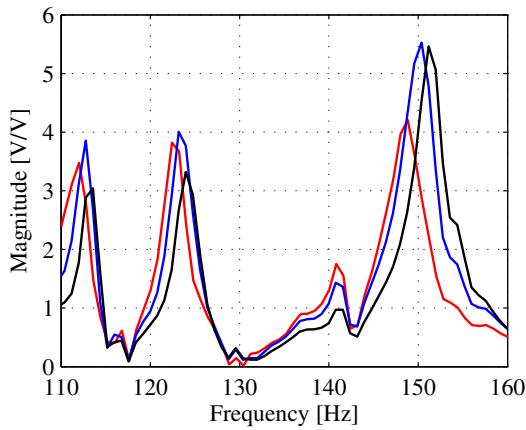


Fig. 4. Actuator FRF measured at different current amplitudes: 0.6 A (black), 1.2 A (blue), 2 A (red).

2.2 Actuator Controller

As mentioned before, the actuator nonlinearity causes a dependence of the structural frequency response on the amplitude of the driving current, that makes the actuator difficult to use in the vibration control system. Therefore, the low-level control objective is to reduce alterations of the structural response due to variations of the input current level.

First of all, a linear model reproducing the behaviour of the actuator mounted to the structure in the neighborhood of a given working condition, i.e. with a given current amplitude, is identified using a frequency domain identification procedure (Kollár, 1993). It can be written in the classical state-space form as

$$\dot{x}_a = A_a x_a + B_a u \quad (1)$$

$$y_a = C_a x_a + D_a u \quad (2)$$

where u is the actuator input current (which will be computed by the vibration controller) and y_a is the measured Bragg signal.

The adopted control strategy is based on a model-following approach (Balestrino et al., 1984) and the control scheme is reported in Fig. 5, as the subsystem inside the orange frame. The characteristic of the model-following algorithm consists in preserving the nature of the input signal which has to be computed by the outer control loop. This makes the use of the actuator more transparent in the higher level control system computing the reference current as a result of an outer feedback loop. This is accomplished by defining a reference model whose input is just the reference current $u_r = u$ while the total actuator current is the sum of the reference current and a corrective current u_c computed by the controller on the basis of the error $e_y = y_a - y_r$ between the actual displacement y_a and the reference displacement y_r . In particular, the reference model is selected equal to the linear model identified as above, i.e.

$$\dot{x}_r = A_a x_r + B_a u_r \quad (3)$$

$$y_r = C_a x_r + D_a u_r \quad (4)$$

As a consequence, it is easy to verify that the dynamics of the state error $e_x = x_a - x_r$ is described by the state space representation

$$\dot{e}_x = A_a e_x + B_a u_c \quad (5)$$

$$e_y = C_a e_x + D_a u_c \quad (6)$$

Since the state e_x is obviously not accessible, the controller is designed according to a standard LQG procedure consisting of a Kalman filter as observer of the error dynamics and an optimal state feedback regulator. Therefore, its dynamic equations can be written in the form

$$\dot{x}_c = A_c x_c + B_c e_y \quad (7)$$

$$u_c = C_c x_c \quad (8)$$

where $A_c = A_a - LC_a - B_a F + LD_a F$, $B_c = L$ and $C_c = -F$, with L and F being the solutions of the two classical Riccati equations.

2.3 Vibration Controller

The high-level controller has been designed considering the structure with the controlled actuator as a standard control problem framework depicted in Fig. 5. In this figure, P is the system to control in the cyan frame, K the controller (green frame) and the transfer function from the generalized disturbance w to the generalized output z is given by the lower LFT (Linear Fractional Transformation) $\mathcal{F}_l(P, K)$ and denoted by T_{zw} .

The vibration controller has been designed on the basis of an optimal control strategy presented in Cavallo et al. (2008) for a MIMO (Multi Input Multi Output) square system, i.e. it has as many (control) inputs as outputs. In particular, assume that in the system P the control inputs and measured outputs have been suitably scaled Maciejowski (1989), so that it can be described by

$$\dot{x} = Ax + B_w w + B_u u \quad (9)$$

$$z = C_z x + D_z u \quad (10)$$

$$y = C_y x + D_{yw} w \quad (11)$$

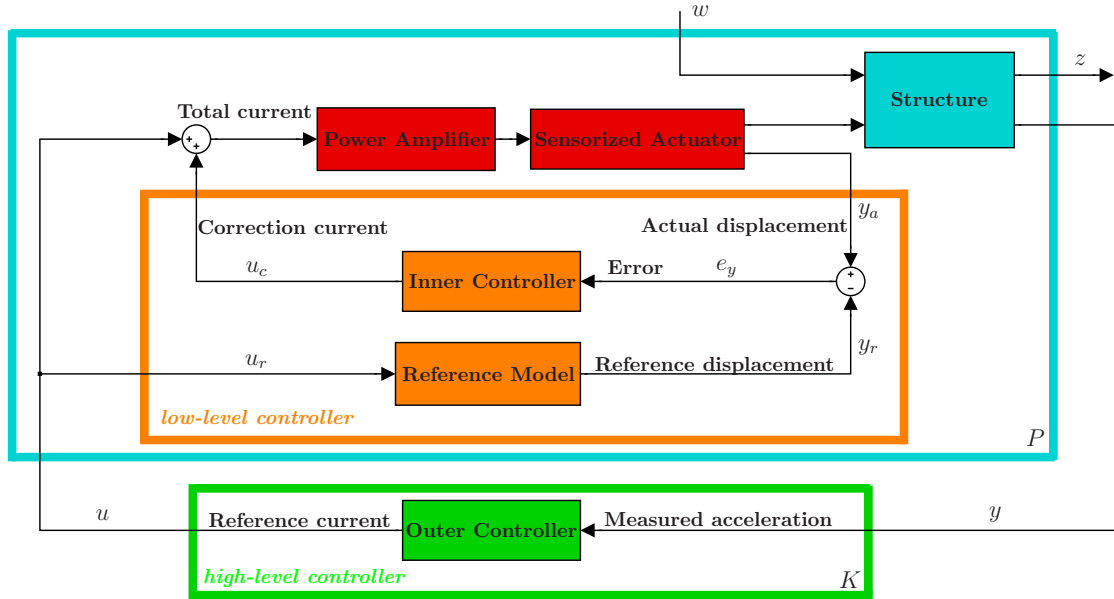


Fig. 5. Advanced control scheme for vibration control.

where

$$D_{zu} = \begin{pmatrix} 0 \\ I \end{pmatrix}, D_{yw} = (0 \ I) \quad (12)$$

$x = (x_1^T \ x_2^T)^T \in \mathbb{R}^{2n}$ is the state vector, $u \in \mathbb{R}^m$ the control input, $y \in \mathbb{R}^m$ the measured (control) output, $w \in \mathbb{R}^{n+m}$ the disturbance (state and measurement disturbances), $z \in \mathbb{R}^{n+m}$ the performance output.

The model describes the dynamics of mechanical systems with n degrees of freedom and, if n is high enough, is a good approximation of infinite-dimensional flexible systems. More specifically, it is well known that a flexible system can be described by a system of PDE's with suitable boundary conditions. By using model order truncation techniques, e.g. FEM strategies, the PDE's can be translated into a finite number of ODE's Meirovitch (1990). By resorting to the "modal coordinates" the following description is obtained Junkins and Kim (1993).

$$A = \begin{pmatrix} 0 & I \\ -\Omega & -\Lambda \end{pmatrix}, \quad (13)$$

$$B_w = \begin{pmatrix} 0 & 0 \\ B_{2w} & 0 \end{pmatrix}, B_u = \begin{pmatrix} 0 \\ B_{2u} \end{pmatrix}, \quad (14)$$

$$C_z = \begin{pmatrix} 0 & B_{2w}^T \\ 0 & 0 \end{pmatrix}, \quad (15)$$

$$C_y = (0 \ B_{2u}^T), \quad (16)$$

where

$$\Omega = \text{diag}(\omega_1^2, \dots, \omega_n^2), \Lambda = \text{diag}(2\zeta_1\omega_1, \dots, 2\zeta_n\omega_n) \quad (17)$$

In this case x_1 are the modal coordinates and x_2 the modal velocities. Moreover, assuming velocity measurement available, the output matrix has the form (16). The choice of the disturbance matrix B_w has a physical justification, i.e. the relationship between modal coordinates and velocities is not subject to uncertainties or perturbations, thus the first n rows of B_w are zero. Also the selection of the

matrix C_z has a physical interpretation, since in noise and vibration reduction, the focus is on the velocity reduction, rather than on modal coordinates control.

A selection of the disturbance matrix is proposed in order to design a strongly stabilizing \mathcal{H}_∞ controller with a set of m zeros at the origin, so as to guarantee bandpass properties to the controller. Let

$$B_{2w} = (\alpha\Lambda + B_{2u}B_{2u}^T)^{1/2} \quad (18)$$

where $\alpha > 0$ is a scalar coefficient to be suitably selected.

The matrix B_w resulting from (14), (18) is composed of two terms: the one weights disturbances in the range of B_u , while the other tries to consider also off-range terms, in particular by weighting the system natural modes. Note that all the modes are weighted, and thus \mathcal{H}_∞ design will try to reduce structural peaks due to vibration modes and to increase robustness with respect to matched disturbances (i.e. in the range of the control input matrix).

Before discussing the solution of the \mathcal{H}_∞ problem, consider the characterization of controllers with bandpass capabilities. The following Theorem addresses this issue.

Theorem 1. With reference to the system (9)-(16), assume that a realization of the controller $K(s)$ is

$$\dot{x}_c = A_c x_c + B_c y \quad (19)$$

$$u = C_c x_c \quad (20)$$

where

$$A_c = A + a\tilde{B}\Upsilon^{-1} + b\Upsilon\tilde{B} \quad (21)$$

$$B_c = c\Upsilon B_u \quad (22)$$

$$C_c = dB_u^T \Upsilon^{-1} \quad (23)$$

and $a, b, c \neq 0, d \neq 0$ are real scalars, $\tilde{B} = B_u B_u^T$ and Υ is a symmetric positive definite matrix. If Υ is chosen as

$$\Upsilon = \begin{pmatrix} \Upsilon_1 & 0 \\ 0 & \Upsilon_2 \end{pmatrix} \quad (24)$$

with $\Upsilon_1, \Upsilon_2 \in \mathbb{R}^{n \times n}$ then K has m zeros in 0.

Based on the above results, an \mathcal{H}_∞ controller is derived with bandpass frequency shape. Moreover, the controller is also stable, as stated by the following Theorem.

Theorem 2. Consider the system (9)-(17), with B_w chosen as in (18). Then, the following controller is strongly stabilizing

$$K_\infty(s, \gamma) = -\frac{\gamma^2}{\gamma^2 - 2} B_u^T (sI - A_\infty)^{-1} B_u \quad (25)$$

where

$$A_\infty = \begin{pmatrix} 0 & I \\ -\Omega & -\Lambda_\infty \end{pmatrix} \quad (26)$$

and

$$\Lambda_\infty = \left(1 - \frac{2}{\gamma^2}\right) \Lambda + 2 \frac{\gamma^2 - 1}{\gamma^2 - 2} \sqrt{\frac{\gamma^2 - 1}{\gamma^2}} B_{2u} B_{2u}^T. \quad (27)$$

Moreover, if

$$\alpha = 2\sqrt{1 - \gamma^{-2}} \quad (28)$$

is considered in (18), then the LFT T_{zw} satisfies

$$\|T_{zw}\|_\infty < \gamma \quad (29)$$

and, $\inf \gamma = \sqrt{2}$.

The proofs of both theorems can be found in (Cavallo et al., 2008).

3. EXPERIMENTAL RESULTS

This section reports the results of the experiments carried out to test the effectiveness of the advanced control system for vibration reduction of flexible structures. The control strategy has been applied to reduce the vibrations of a real aeronautical structure, i.e. a fuselage skin panel of a BOEING 717. The panel is stiffened by two bulkheads and three orthogonal stiffeners rivetted to the rear of the panel itself and has been suspended by a couple of soft springs to simulate the free boundary conditions. The actuator has been mounted to a stiffener by removing a rivet; the output acceleration is measured by means of an accelerometer by PCB placed on the rear part of the panel in correspondence with the actuator mounting point (co-located case). The control algorithm has been digitally implemented by using a dSPACE rapid prototyping real-time control system with 16-bit A/D channels and 14-bit D/A channels at a sampling frequency of 20 kHz.

As the first step of the design procedure, the linear model in Eqs (1),(2) has been identified by resorting to the FDIDENT Matlab Toolbox, resulting in a 24th order system. Using this system as reference model, the LQG controller in Eqs. (7),(8) has been designed experimentally tuning the weighting matrices of the Riccati equations. In order to verify the effect of the designed controller, the following indicator has been defined to compare the FRFs estimated at two different levels of the input current

$$E(\omega) = |H_{0.6}(j\omega) - H_{1.2}(j\omega)| \quad (30)$$

where $H_{0.6}(j\omega)$ and $H_{1.2}(j\omega)$ are the FRFs measured with an amplitude of the input chirp current signal equal to

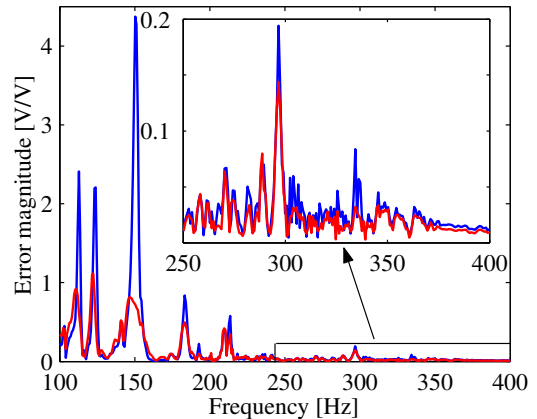


Fig. 6. Indicator $E(\omega)$ defined in Eq. (30) with actuator controller switched off (blue) and on (red).

0.6 A and 1.2 A respectively. The results are shown in Fig. 6 reporting the indicator E evaluated with the actuator controller switched off and on. For the whole frequency range the indicator assumes lower values when the actuator controller is activated, meaning that the alteration of the structural response due to the nonlinearity of the actuator is significantly reduced.

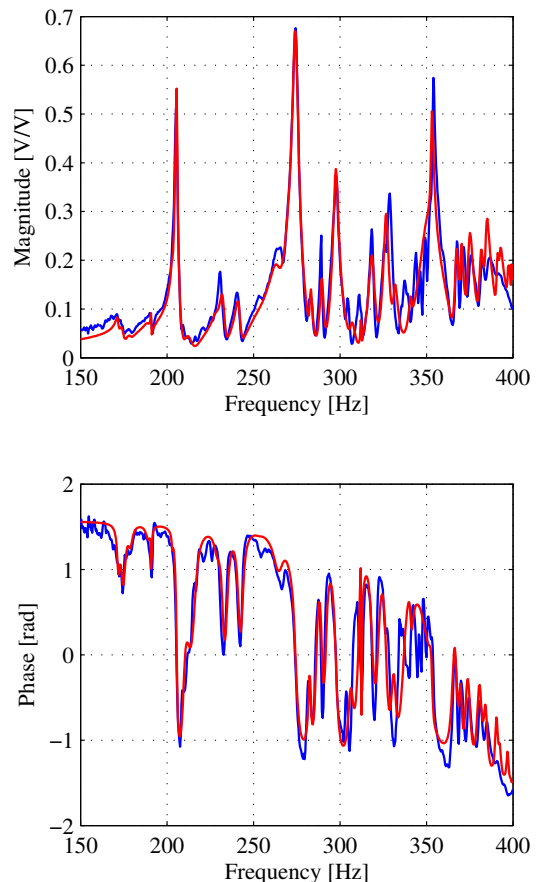


Fig. 7. Experimental identification of the structure: measured FRF (blue) and modelled FRF (red)

The second step of the design procedure is devoted to identify a model of the plant P in Eqs. (9)–(11) necessary for computing the \mathcal{H}_∞ vibration controller in Eqs. (25)–

(27) presented in Section 2.3. By applying the gray-box identification procedure specifically devised for flexible structures proposed by Cavallo et al. (2007), a model with 35 modes has been estimated whose FRF is compared to the measured FRF in Fig. 7. Choosing the value 1.5 for the design parameter γ in Eq. (29), the resulting controller has been implemented on the dSPACE system. The complete advanced control system has been tested considering the four case studies obtained by combining the ON/OFF states of the low-level (inner) and the high-level (outer) controllers. In Fig. 8 the magnitude of the FRF from the input disturbance to the measured acceleration is reported in the four case studies. As expected, the higher values correspond to the open loop (Inner OFF/Outer OFF) case, while the better disturbance rejection (vibration reduction) is obtained when both feedback controllers are active (Inner ON/Outer ON), with a reduction of 14.4 dB of the infinity norm.

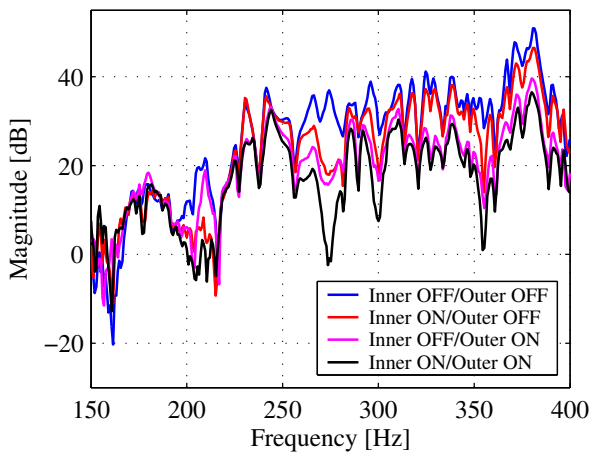


Fig. 8. Experimental results for the two-level control scheme.

4. CONCLUSION

The presented control solution for a vibration reduction problem can be referred to as an advanced control system from a twofold point of view. It exploits an unconventional actuation system constituted by a smart actuator with an integrated optical sensor and it is based on a multi-loop control architecture, where the inner controller is aimed at linearizing the actuator behaviour and the outer loop is devoted to reject the broadband disturbance acting on the structure. The experiment has been conducted on a relatively small scale test article using only one actuator just to prove the control concept, and owing to the good results, the implementation of the system on a full scale test article (fuselage segment of a civil aircraft) using a large number of actuators has been agreed by the project consortium and is already in progress.

ACKNOWLEDGEMENTS

This paper was supported partially by the MESEMA project, funded under the 6th FP of the EC (Contract N. AST3-CT-2003-502915) and partially by the PRIN 2005 project funded by MIUR (Contract N. 2005097135-003).

REFERENCES

- M.J. Balas. Trends in large space structure control theory: Fodest hopes, widest dreams. *IEEE Transactions on Automatic Control*, 27(3):522–535, 1982.
- A. Balestrino, G. De Maria, and A. S. I. Zinober. Nonlinear adaptive model-following control. *Automatica*, 20(5):559–568, 1984.
- D.U. Campos-Delgado and Zhou K. A parametric optimization approach to \mathcal{H}_∞ and \mathcal{H}_2 strong stabilization. *Automatica*, 39:1205–1211, 2003.
- A. Cavallo, G. De Maria, Natale. C., and S. Pirozzi. Gray-box identification of continuous-time models of flexible structures. *IEEE Transactions on Control Systems Technology*, 15(5):967–981, 2007.
- A. Cavallo, G. De Maria, Natale. C., and S. Pirozzi. Robust control of flexible structures with stable \mathcal{H}_∞ and \mathcal{H}_2 bandpass controllers. *Automatica*, doi:10.1016/j.automatica.2007.10.020, 2008.
- S. Gümüşsoy and H. Özbay. Remarks on strong stabilization and stable \mathcal{H}_∞ control design. *IEEE Transactions on Automatic Control*, 50(12):2083–2087, 2005.
- Y. Halevi. Stable lqg controllers. *IEEE Transactions on Automatic Control*, 39(10):2104–2106, 1994.
- J.L. Junkins and Y. Kim. *Introduction to dynamics and control of flexible structures*. AIAA Education Series, Washington DC, 1993.
- A. D. Kersey, M. A. Davis, H. J. Patrick, M. LeBlanc, K. P. Poo, A. G. Askins, M. A. Putnam, and E. J. Friebele. Fiber grating sensors. *Journal of Lightw. Technol.*, 15(8):1442–1462, 1997.
- I. Kollár. On frequency-domain identification of linear systems. *IEEE Transactions on Instrumentation and Measurements*, 42(1):2–6, 1993.
- L. Lecce, E. Monaco, and F. Franco. Mesema (magnetoelastic energy system for even more electric aircraft): Objectives and first results. In *Proc. 10th International Conference on New Actuators*, pages 936–939, Bremen, Germany, 2006.
- J.M. Maciejowski. *Multivariable Feedback Design*. Addison-Wesley, Wokingham, 1989.
- C. May, K. Kuhnen, and H. Pagliarulo, P. and Janocha. Magnetostrictive dynamic vibration absorber (dva) for passive and active damping. In *Proc. 5th European Conf. on Noise Control*, pages 1–6, Naples, Italy, 2003.
- C. May, A. Minardo, Natale. C., P. Pagliarulo, and S. Pirozzi. Modelling and control of a smart auxiliary mass damper equipped with a bragg grating. In *2007 IEEE/ASME International Conference on Advanced Intelligent Mechatronics*, Zurich, 2007.
- C. May, P. Pagliarulo, and H. Janocha. Optimisation of a magnetostrictive auxiliary mass damper. In *Proc. 10th International Conference on New Actuators*, pages 344–348, Bremen, Germany, 2006.
- L. Meirovitch. *Dynamic and Control of Structures*. Wiley-Interscience Publication, New York, 1990.
- S. Skogestad and I. Postlethwaite. *Multivariable Feedback Control: Analysis and Design, (2nd Ed.)*. John Wiley and Sons, New York, 2005.
- D.C. Youla, J.J. Bongiorno, and C.N. Lu. Single-loop stabilization of linear multivariable plants. *Automatica*, 10:159–173, 1974.